

## RESEARCH ARTICLE

Editorial Process: Submission:02/10/2022 Acceptance:08/11/2022

***In Vitro* Study on Effect of Zinc Oxide Nanoparticles on the Biological Activities of *Croton tiglium* L. Seeds Extracts****Wael Mahmoud Aboulthana<sup>1\*</sup>, Nagwa Ibrahim Omar<sup>1</sup>, Amal Mohamed El-Feky<sup>2</sup>, Enas Ahmed Hasan<sup>3</sup>, Noha El-Sayed Ibrahim<sup>4</sup>, Ahmed Mahmoud Youssef<sup>5</sup>****Abstract**

**Objective:** *Croton tiglium* L. seeds were studied against colon cancer induced chemically in rats after incorporating silver nanoparticles (Ag-NPs) but the body has no the ability to discrete silver or silver ions. Therefore, the present study was designed to reveal the biological activities of different *C. tiglium* L. seeds extracts incorporated with zinc oxide nanoparticles (ZnO-NPs). **Results:** It was found that *C. tiglium* L. seeds provided with high contents of total protein (27.43 g/100g), carbohydrate (18.29 g/100 g) and lipid (46.31 g/100 g). The chromatographic techniques revealed that concentrations of the predominant compounds increased in all studied extracts (ethanolic, aqueous and petroleum ether) after incorporating ZnO-NPs. The *in vitro* biological activities showed that the aqueous extract possessed the highest antioxidant and scavenging activities. It exhibited the highest inhibitory effect on  $\alpha$ -amylase (41.89%) and acetyl cholinesterase (AChE) (23.00%) in addition to its higher anti-arthritis activity. All the biological activities increased after incorporating ZnO-NPs. It showed the highest cytotoxic activity that increased after incorporating ZnO-NPs against human colon carcinoma (CACO-2) cells. Therefore, this extract was selected for undergoing further studies on CACO-2 cells. The aqueous extract incorporated with ZnO-NPs arrested growth of CACO-2 cells at G2/M and increased percentage of total apoptotic cells and necrosis. The median lethal dose (LD<sub>50</sub>) showed that the extracts incorporated with ZnO-NPs were safer than the native extracts. **Conclusion:** The study showed that the aqueous extract was the most active extract that consequently exhibited promising biological activities after incorporating ZnO-NPs.

**Keywords:** *Croton tiglium* Seeds- Zinc oxide nanoparticles- Green Nanotechnology- Biological Activity- Toxicity*Asian Pac J Cancer Prev*, **23** (8), 2671-2686**Introduction**

*Croton tiglium* L. is categorized as the second largest genus under the Family “*Euphorbiaceae*”. Approximately 1300 species of largely trees, shrubs and herbs that grow under varied environmental conditions in tropical and sub-tropical regions were belonged to this large genus (Torres et al., 2008). Due to the presence of essential oils, the leaves, seeds, stem, roots, and the juice from the bark were widely utilized for medicinal and nutritional purposes among different global communities (Harkat-Madouri et al., 2015; Sai Prassana and Karpaga, 2015). Hu et al., (2010) emphasized that *C. tiglium* L. seeds are rich in phorbol esters, crotonic acid and fatty acids in addition to active phytoconstituents that are responsible for severe purgative effect of the *C. tiglium* L. seeds extract. Due to the strong toxic effect of the chemical synthetic products,

components of natural essential oil are gaining frequent presence and increasing interest in the recent studies investigating their potential activity and functional utility (Babahmad et al., 2018; Rakmai et al., 2018). These essential oils possessed purgative, analgesic, antibacterial, anti-oxidation, anti-inflammatory and anti-tumor activities. Therefore, they are abundantly utilized in cosmetic industries and indigenous medicines (El Gendy et al., 2015). It was reported that linoleic acid, oleic acid and eicosenoic acid are the most abundant fatty acids exist in a methyl-esterified sample obtained by reflux method (Mei et al., 2012). It increases gastrointestinal motility, has a soothing effect on skin, reduces inflammation, expectorant and rubefacient. Traditionally, *C. tiglium* L. is used for kidney stones, bronchial irritation, convulsions and skin disorders. It has been utilized widely among the Asian communities for treating gastrointestinal problems

<sup>1</sup>Biochemistry Department, Biotechnology Research Institute, National Research Centre, 33 El Bohouth St. (Former El Tahrir St.), P.O. 12622, Dokki, Giza, Egypt. <sup>2</sup>Pharmacognosy Department, National Research Centre, 33 El Bohouth St. (Former El Tahrir St.), P.O. 12622, Dokki, Giza, Egypt. <sup>3</sup>Egyptian Organization for Biological Products & Vaccines (Vacsera), Giza, Egypt. <sup>4</sup>Microbial Biotechnology Department, Biotechnology Research Institute, National Research Centre, 33 El Bohouth St. (Former El Tahrir St.), P.O. 12622, Dokki, Giza, Egypt. <sup>5</sup>Packaging Materials Department, National Research Centre, 33 El Bohouth St. (Former El Tahrir St.), P.O. 12622, Dokki, Giza, Egypt. \*For Correspondence: wmkamel83@hotmail.com

(Ojo et al., 2017).

Development of nanotechnology led to astonishing distribution in progression of medicine and health care system. The mechanism by which the metal nanoparticles (M-NPs) were synthesized using plant extracts by mean of green nanotechnology may be associated with concept of the phytoremediation (Selvarajan and Mohanasrinivasan, 2013). It is well known that silver nanoparticles (Ag-NPs) are utilized widely as an effective antimicrobial agent coating on catheter and wound dressing (Konop et al., 2016). There is no clear regulation enough for managing risk of the Ag-NPs in implant medical devices. On the other side, the human body has no the ability to discrete silver or silver ions, leading to an accumulation of silver as well as destruction of DNA and / or red blood cells (Chen et al., 2015 ; Ferdous and Nemmar, 2020).

As reported by Aboulthana et al., (2019), aqueous *C. tiglium* L. seeds (the most effective) extract used for green synthesis of Ag-NPs. Although the silver *C. tiglium* L. nano-extract showed ameliorative effect against colon cancer induced chemically in rats as demonstrated by Aboulthana et al., (2020), Aboulthana et al., (2021) postulated that incorporating Ag-NPs into aqueous *C. tiglium* L. seeds extract caused deleterious effect on brain tissue when administrated orally due to its high affinity to accumulate in the brain affecting the enzymatic and non-enzymatic antioxidant system. Zinc oxide (ZnO) or zinc oxide nanoparticles (ZnO-NPs) differ from the other metal oxides. They are characterized by their biodegradability, low toxicity and economy. Therefore, they are approved by Food and Drug Administration (FDA) in the past two decades to be utilized in biomedicine applications, especially in discipline of antibacterial or anticancer fields in addition to its utilization in the industrial products such as coating, paint and cosmetics (Parihar et al., 2018). Many recent studies demonstrated that ZnO-NPs are characterized by good biocompatibility and antibacterial properties (Ozkan et al., 2018 ; Jiang et al., 2018 ; Hameed, 2018). The ZnO-NPs that were prepared by the chemical and physical methods are not suitable to be utilized in the medical field due to limitation of chemical reagents as well as their residue after reaction. Development of green chemistry has attracted more attention because it is believed to be biocompatible, nontoxic and eco-friendly. Many recent studies proved that green technology-based synthesis of nanoparticles is considered as promising methods for large-scale production of M-NPs to be utilized for biomedical applications. Results of the recent studies proved that the ZnO-NPs that were biosynthesized using a wide variety of plant extracts are safe for human use alternative to Ag-NPs or other M-NPs (Song and Yang, 2016 ; Ali et al., 2016 ; Ji et al., 2017). The current experiment was designed to reveal the biological activities of different *C. tiglium* L. seeds extracts after incorporating ZnO-NPs.

## Materials and Methods

### *Determination of nutritional value of C. tiglium L. seeds*

Total protein content was estimated in *C. tiglium* L.

seeds by micro-kjeldahl method as stated by El-Feky et al., (2020). Total carbohydrate content was quantified as glucose by phenol sulfuric acid method suggested by El-Feky et al., (2018). Total lipid content was gravimetrically determined based on the method suggested by AboulNaser et al., (2020). Consequently, the obtained values (proteins, carbohydrates and lipids) were used for calculating the caloric value of *C. tiglium* L. seeds using the equation suggested by Coelho et al., (2014).

### *Preparation of different plant extracts*

*C. tiglium* L. seeds were obtained from Agricultural Research Center, Giza, Egypt. The crushed dried seeds were successively extracted in soxhlet apparatus with petroleum ether (60 - 80°C), ethyl alcohol, and then with distilled water for 20 hrs for each solvent, the obtained three extracts were separately filtered then concentrated in a rotary evaporator at 45°C under reduced pressure to dryness.

### *Isolation and identification of the major compounds from different C. tiglium seeds L. extracts*

The petroleum ether extract was chromatographed on silica gel column. Elution was successively carried out by methylene dichloride (CH<sub>2</sub>Cl<sub>2</sub>) and increasing the polarity with ethyl acetate. The fractions were successively collected and individually concentrated to 5 ml then screened by thin layer chromatography (TLC) using toluene : ethyl acetate (7:3 v/v) as solvent system. The separated fractions were visualized by spraying with 10% H<sub>2</sub>SO<sub>4</sub> and heating at 110°C for 5 min. The resulting similar fractions were collected from the column together according to R<sub>f</sub> values. Structures of the isolated compounds were interpreted based on the spectral analyses (FT-IR, 1H-NMR, 13C-NMR and Mass spectroscopy).

The ethanolic extract was applied on preparative TLC using chloroform: methanol (80:20 and 70:30 v/v) as developing system. The plates were examined under the UV light at 254 and 366 nm, respectively. The selected bands were scratched and collected. The R<sub>f</sub> values of the isolated compounds were recorded and the structural elucidation of the isolated compounds were interpreted based on their spectral analyses (UV, MS, IR, 1H-NMR and 13C-NMR spectrometry).

### *Preparation of zinc oxide C. tiglium L. seeds nano-extract*

ZnO-NPs were synthesized using plant extracts as reducing agents in order to prepare ZnO-NPs with optimum yield and particle size. For preparation of ZnO-*C. tiglium* seeds nano-extract, the ZnO-NPs were synthesized by sol-gel method suggested by Bao et al., (2012) with some modifications. The plant extract was added into zinc acetate solution till obtaining the white precipitate that dried then converted into powder to be ready for characterization.

### *Characterization of the biosynthesized zinc oxide nanoparticles*

The ZnO-NPs spectra were assayed by Shimadzu UV-VIS recording spectrophotometer UV-240 at λ 200 - 800 nm after diluting the samples (10-fold) with

deionized water. The crystalline nature and grain size of the synthesized ZnO-NPs were analyzed by a Philips X-Ray Diffractometer (XRD) (PW 1930 generator, PW 1820 goniometer) equipped with Cu K $\alpha$  radiation as an X-ray source (45 kV, 40 mA, with  $\lambda = 0.15418$  nm). Shape and size of the synthesized ZnO-NPs were determined at high resolution level (200 KV) using Transmission Electron Microscope (TEM) (model JEM-1230, Japan) operated at accelerating voltage of 120 kV, with maximum magnification of 600X103 and a resolution until 0.2 nm. The average hydrodynamic size of the synthesized ZnO-NPs was determined by Dynamic Light Scattering (DLS) (Malvern Zetasizer Nano ZS, Malvern Instruments Ltd., Malvern, United Kingdom) according to method suggested by Murdock et al., (2008).

### Determination of the phyto-constituents in *C. tiglium* L. seeds extracts before and after incorporating zinc oxide nanoparticles

#### 1. Quantitative determination of major phyto-constituents

Concentration of total polyphenols was determined using Folin Ciocalteu reagent according to method suggested by Singleton and Rossi (1965). Total tannins contents were determined using tannic acid as a reference compound based on the method described by Broadhurst and Jones (1978).

#### 2. Investigation of the lipoidal constituents

The P. ether extracts of *C. tiglium* L. seeds before and after incorporating ZnO-NPs were subjected to gas chromatograph coupled with a mass spectrometer (GC/MS analysis) (model Shimadzu GC/MS–QP5050A) on an Agilent 6890, 70 eV. MS spectrometer; Finnigan Model 3200, Mass spectrometer at 70 eV. The constituents have been identified by comparison of their spectral fragmentation patterns with those of the available database libraries Wiley (Wiley Int.) USA and NIST (Nat. Inst. St. Technol., USA) and/or published data. Quantitative determination was carried out based on integration of the area under peak according to the method suggested by Elswawi et al., (2020).

#### 3. Investigation of the phenolics and flavonoidal compounds

The different phenolic and flavonoidal compounds were identified in the aqueous and ethanolic extracts of *C. tiglium* L. seeds before and after incorporating ZnO-NPs using high pressure liquid chromatography (HPLC) (Shimadzu-UFLC Prominence) equipped with an auto sampler (Model-SIL 20AC HT) and UV-Vis detector (Model-SPD 20A) (Japan). The separation process was carried out through analytical column of an Eclipse XDBC18 (150 X 4.6  $\mu$ m; 5  $\mu$ m) with a C18 guard column (Phenomenex, Torrance, CA). The mobile phase is consisting of solvent system of acetonitrile (solvent A) and 2% acetic acid in water (v/v) (solvent B). Before the chromatographic run, all samples were filtered through a 0.45  $\mu$ m Acrodisc syringe filter (Gelman Laboratory, MI). Each sample (50  $\mu$ l) was injected automatically by the injector piece. The flow rate was kept at 0.8 m min<sup>-1</sup> for a total run time of 70 min and the gradient program was

as follows: 100% B to 85% B in 30 min, 85% B to 50% B in 20 min, 50% B to 0% B in 5 min and 0% B to 100% B in 5 min. The peaks were monitored simultaneously at 280 and 320 nm for the benzoic acid and cinnamic acid derivatives, respectively. When the chromatographic run was finished, the peaks were identified by congruent retention times and UV spectra and compared with those of the standards (El-Sayed et al., 2018).

### In vitro study on different *C. tiglium* L. seeds extracts before and after incorporating zinc oxide nanoparticles

#### 1. Antioxidant activity

Total antioxidant capacity (TAC) and total iron reducing power were assessed according to the methods suggested by Prieto et al., (1999) and Oyaizu (1986), respectively. The scavenging activities were assessed against 1,1-Diphenyl-2-picryl-hydrazyl (DPPH) and 2,2'-azinobis-(3-ethylbenzothiazoline-6-sulfonic acid) (ABTS) radicals according to the methods suggested by Rahman et al., (2015) and Arnao et al., (2001), respectively.

#### 2. $\alpha$ -amylase inhibitory assay

It was carried out using acarbose as standard drug for calculating percentage of  $\alpha$ -amylase inhibition (%) using 3,5-dinitrosalicylic acid (DNSA) method (Wickramaratne et al., 2016).

#### 3. Acetyl cholinesterase (AChE) enzyme activity

It was measured for calculating percentage of AChE inhibition (%) using Ellman's method (Ellman et al., 1961).

#### 4. Antiarthritic activity

##### 4.1. Protein denaturation

Percentage of protein denaturation inhibition can be calculated according to the method described by Lavanya et al., (2010) and Das and Sureshkumar (2016). All results were compared with standard (diclofenac sodium) and the control represents 100% protein denaturation.

##### 4.2. Proteinase inhibitory activity

This assay was carried out by calculating percentage of the proteinase inhibitory activity according to the method suggested by Oyedapo and Famurewa (1995).

#### 5. Cytotoxic activity

Cytotoxic activities were determined against human hepatocellular (HEPG-2) and colon carcinoma (CACO-2) cells using 3-(4,5-dimethylthiazol-2-yl)-2,5-diphenyl tetrazolium bromide (MTT) assay as suggested by Vichai and Kirtikara (2006). Percent of cell-growth inhibition (%) and median inhibitory concentration (IC<sub>50</sub>) were calculated using IC<sub>50</sub> calculation software.

#### 6. DNA content analysis

The CACO-2 cells (3 $\times$ 10<sup>5</sup>/well) were seeded into 6-well plates, cultured overnight and treated with different *C. tiglium* L. extracts and their ZnO nano-extracts individually for 24 hrs. The cells were fixed in 75% ethanol at -4°C overnight then incubated with 50 ng/mL PI staining

solution and 0.1 mg/mL RNase A in dark place at room temperature for 15 min. The DNA content was quantified in the cells by flow cytometry (BD FASCCalibur-USA).

### 7. Cell apoptosis

The cell apoptosis was assessed by Annexin V-FITC apoptosis detection kit (Annexin V-FITC-BD Bioscience Pharmingen™, USA). The CACO-2 cells ( $3 \times 10^6$ /well) were seeded into 6-well plates then cultured overnight before the exposure to different concentrations of *C. tiglium* L. extracts and their ZnO nano-extracts (50, 100, 150, 200  $\mu\text{g/ml}$ ). Furthermore, both of each extract and its ZnO nano-extract (100 $\mu\text{g/ml}$ ) added to CACO-2 cells for different times (24, 36, 48 and 48 hrs). Cells were collected by cold centrifugation at 300 x g for 10 min and consequently washed twice and re-suspended in 500  $\mu\text{l}$  of cold (+4°C) 1X PBS buffer then precipitated again by centrifugation. This step was followed by adding 100  $\mu\text{l}$  1X Binding Buffer per sample. Annexin V (100  $\mu\text{l}$ ) was added to treated cell samples (106 cell/ml) then incubated. Annexin V-FITC (5 $\mu\text{l}$ ) and propidium iodide (PI) (5 $\mu\text{l}$ ) were incubated in the dark for 15 min. at room temperature, then 400  $\mu\text{l}$  of 1X binding buffer was added. The cells were immediately analyzed by flow cytometry (BD FASCCalibur-USA) within 1hr for a maximal signal (Koopman et al., 1994).

### 8. Extraction of RNA and quantitative RT-PCR

The CACO-2 cells were cultured in six-well plates and exposed individually to *C. tiglium* L. extracts and their ZnO nano-extracts (100  $\mu\text{g/ml}$ ). Total RNAs were extracted from treated cells using the RNeasy Mini Kit (Qiagen RNA extraction/BioRad syber green PCR MMX) based on the method suggested by Pfaffl (2001). For quantifying expressions of EGFR, Bcl-2 and Casp3 genes, the total RNAs (10 ng) from each sample was processed by reverse transcription for cDNA synthesis using the High Capacity cDNA Reverse Transcriptase kit (Applied Biosystems, USA). Consequently, the cDNA was amplified with the Syber Green I PCR Master Kit (Fermentas) in a 48-well plate using the Step One instrument (Applied Biosystems, USA), as a following: 10 min at 95°C for enzyme activation followed by 40 cycles of 15 sec at a temperature of 95°C, 20 sec at 55°C and 30 sec at 72°C for the amplification step. The changes in expression of each target gene were normalized relative to the mean critical threshold (CT) values of GAPDH as a housekeeping gene by the  $\Delta\text{Ct}$  method. One  $\mu\text{l}$  of both primers specific for each target gene (EGFR (F: 5'-GACTCCGTCCAGTATTGATCG-3'; B: 5'-GCCCTTCGCACTTCTTACAATT-3'), Bcl2 (F: 5'-TCCCTCGCTGCACAAATACTC-3'; B: 5'-ACGACCCGATGGCCAAGA-3'), Casp3 (F: 5'-TGTTTGTGTGCTTCTGAGCC-3'; B: 5'-CACGCCATGTCATCATCAAC-3') and GAPDH (F: 5'-GAAGGTGAAGGTTCGGAGTCA-3'; B: 5'-TTGAGGTCAATGAAGGGGTC-3')) was added. The mRNA levels were quantified using the  $2^{-\Delta\Delta\text{Ct}}$  method that was suggested by Wang et al., (2014). GAPDH was used as the internal control. Experiments for each gene

were conducted in triplicate.

### Median lethal dose of different extracts ( $LD_{50}$ )

The different native *C. tiglium* L. extracts and their ZnO nano-extracts (after incorporating ZnO-NPs) were studied separately for evaluating the  $LD_{50}$ . Three hundred and twenty four adult albino mice (weight 20-25 g) were divided into 9 groups (6 mice in each group) for calculating the  $LD_{50}$  of the native ethanolic *C. tiglium* L. extract, 9 groups for ZnO ethanolic nano-extract, 9 groups for native aqueous extract, 9 groups for ZnO aqueous nano-extract, 9 groups for native P. ether extract and 9 groups for ZnO P. ether nano-extract. For each extract, the groups were treated orally by stomach tube with rising doses of 1,000, 2,000, 4,000, 6,000, 8,000, 10,000, 12,000, 14,000 and 16,000 mg/Kg. Number of dead mice was recorded after 24 hrs of extract administration. The  $LD_{50}$  was calculated according to the methods suggested by Paget and Barnes (1964).

## Results

### The nutritional composition of *C. tiglium* L. seeds

It was found that *C. tiglium* L. seeds provided great values of total protein (27.43 g/100g), carbohydrate (18.29 g/100 g) and lipid contents (46.31 g/100 g). Consequently, the caloric value of *C. tiglium* L. seeds was calculated as 599.67 kcal/100g.

### The major compounds isolation from different *C. tiglium* L. seeds extracts

The steroidal and terpenoidal compounds were isolated from petroleum ether extract and identified by column chromatography technique. The collected fractions were tested using Liebermann–Burchard reagent, then they were spotted on TLC plate and sprayed with 10%  $\text{H}_2\text{SO}_4$  reagent. The positively tested fractions were applied on TLC silica gel plates against the available authentics. By comparing Rf values and the chromatographic appearance under UV, two steroidal compounds ( $\beta$ -sitosterol and stigmasterol) beside to one pentacyclic triterpenoid ( $\alpha$ -amyrin) were identified and isolated in pure form. Stigmasterol was isolated for the first time from *C. tiglium* L. seeds. It was identified at Rf value 0.20 and obtained as white crystalline powder with melting point 170°C. Furthermore, isopimar-7,15-dien-3 $\beta$ -ol was also isolated by silica gel column with  $\text{CH}_2\text{Cl}_2$ : EtOAc (90:10 v/v) as amorphous powder and identified at Rf value 0.46 in toluene : ethyl acetate solvent system (7:3 v/v). UV  $\lambda_{\text{max}}$  was 226 nm; FT-IR bands at 3320  $\text{cm}^{-1}$  for OH stretching, 2945, 3850  $\text{cm}^{-1}$  for C-H stretching, and 1645 $\text{cm}^{-1}$  for  $\text{C}=\text{C}$  Stretch. EI-MS 70 eV m/z (rel. int.): 288 [M]<sup>+</sup> (10) calculated for molecular formula  $\text{C}_{20}\text{H}_{32}\text{O}$ , 273 [M- $\text{CH}_3$ ]<sup>+</sup> (15), 270 [M- $\text{H}_2\text{O}$ ]<sup>+</sup> (8), 255 (30), 245 (13), 213 (16), 200 (22), 185 (25), 171 (29), 145 (51), 132 (69), 129 (100), 119 (81), 105 (70), 91 (25). As well as, stigmast-4-en-3-one was isolated for the first time from *C. tiglium* L. seeds by silica gel column with  $\text{CH}_2\text{Cl}_2$ -EtOAc (80:20 v/v) as white needles, melting point 155°C. It was identified at Rf value 0.63 in toluene

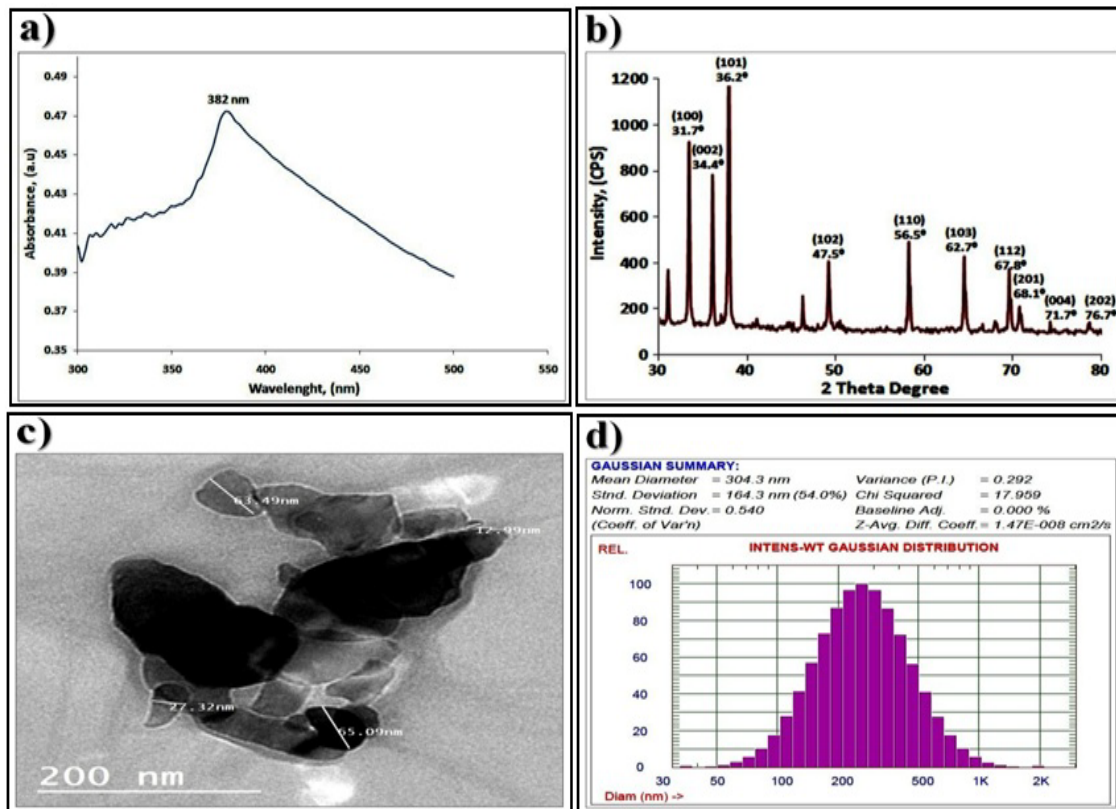


Figure 1. Characterization of the Synthesized Zinc Oxide Nanoparticles (ZnO-NPs) Showing. a) Ultraviolet-visible (UV-VIS) spectrum, b) X-Ray Diffraction (XRD) spectrum, c) Transmission Electron Microscope (TEM) image and d) Dynamic Light Scattering (DLS).

:ethyl acetate solvent system (7:3 v/v). UV  $\lambda_{max}$  was 255 nm; FT-IR bands at 3315  $cm^{-1}$  for OH stretching, 2927, 3810  $cm^{-1}$  for C-H stretching, 1715  $cm^{-1}$  for C=O stretching, and 1,620  $cm^{-1}$  for -C=C- Stretch. EI-MS 70 eV  $m/z$  (rel. int.): 412 (35) calculated for molecular formula C<sub>29</sub>H<sub>48</sub>O, base peak at  $m/z$  124 (100). The characteristic fragmentations were  $m/z$  43 (55), 55 (40), 71 (25), 95 (28), 134 (10), 150 (15), 178 (12), 213 (20), 229 (35), 255 (20), 273 (11), 329 (16), 381 (9), 396 (17).

Quercetin-7-O- $\beta$ -D-glucopyranoside was isolated from ethanolic extract with CHCl<sub>3</sub>: MeOH (80:20 v/v) as yellow crystals with melting point 220°C. It

was identified at R<sub>f</sub> value 0.67 and gave positive test for flavonoids. UV  $\lambda_{max}$  in MeOH (256, 269sh, 372), MeOH+NaOMe (244sh, 291, 366, 456), MeOH+AlCl<sub>3</sub> (258sh, 273, 340, 458), MeOH+AlCl<sub>3</sub>/HCl (268, 303sh, 365, 425) stable UV absorbance was observed in band I and II indicating presence of hydroxyl group at C-3 and C-5, MeOH+NaOAc (286, 377, 428sh), MeOH+NaOAc/H<sub>3</sub>BO<sub>3</sub> (261, 290sh, 385) bathochromic shift of band I indicates the presence of 3', 4' dihydroxy group. 1H-NMR (400 MHz, CD<sub>3</sub>OD,  $\delta$  ppm): 6.45 (1H, d, J=2.8Hz, H-6), 6.79 (1H, d, J=2.8Hz, H-8), 7.90 (1H, d, J=2.7Hz, H-2'), 6.93 (1H, d, J=8.5Hz, H-5'), 7.65 (1H, dd, J=2.7, 8.5Hz,

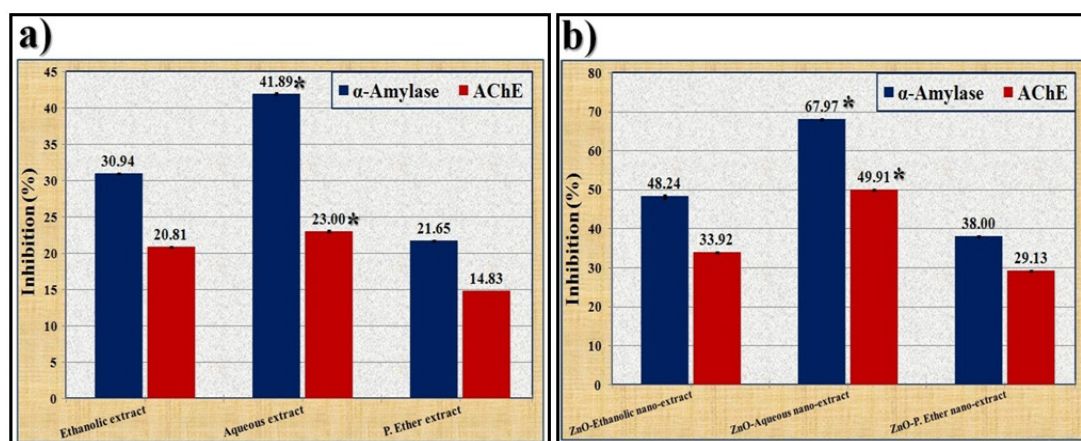


Figure 2. Percent of the Inhibitory Effect on Activities of  $\alpha$ -amylase and Acetyl Cholinesterase (AChE) for a) native *C. tiglium* seeds extracts and b) ZnO-*C. tiglium* L. seeds nano-extracts. Values expressed as mean of three replicates  $\pm$  SE. \* denotes the most effective extract

Table 1. GC/MS Analysis of the Lipoidal Constituents in Petroleum ether *C. tiglium* L. seeds Extract before and after Incorporating ZnO-NPs

Class	Compound	Mol. Weight	BP	Relative area %		
				Before	After	
Hydrocarbons	4-Decene	140	55	0.06	0.07	
	4-Methylnonane	142	41	1.04	1.05	
	9-methyl-1-decene	154	56	0.97	1.11	
	2-Methyldecane	156	43	1.65	2.06	
	5-Methyl-4-undecene	168	55	0.11	0.13	
	2-Methylundecane	170	43	2.03	3.15	
	2,5,6-Trimethyldecane	1 184	57	1.54	2.01	
	2-Methyltridecane	198	43	0.15	0.18	
	2,4,6,8-Tetramethyl-1-undecene	210	43	0.24	0.26	
	2-Methyltetradecane	212	57	1.03	1.05	
	n-Hexadecane	226	43	2.02	2.11	
	n-Heptadecane	240	43	3.34	3.37	
	n-Octadecane	254	57	5.61	6.24	
	6-Methyl octadecane	268	57	2.08	2.22	
	n-Docosane	310	43	3.76	4.09	
	Tetracosane	338	57	6.54	6.57	
	Hentriacontane	436	57	7.04	7.12	
	Fatty alcohols	Hept-4-en-1-ol	114	41	1.98	2.01
		2-Octen-1-ol	128	57	0.93	0.96
2-Nonen-1-ol		142	57	12.25	13.02	
2-Decen-1-ol		156	57	2.08	2.1	
10-Dodecyn-1-ol		182	68	0.98	0.99	
Dodecanol		186	41	1.54	1.57	
Tetradecanol		214	41	1.96	2.02	
6,9-Pentadecadien-1-ol		224	67	1.14	1.14	
Octadecanol		270	41	1.04	1.06	
Aldehydes		2,2-Dimethyl-4-pentenal	112	55	0.87	1.03
	Heptanal	114	57	1.15	1.17	
	2-Isononenal	140	43	1.01	1.04	
	Nonanal	142	41	0.19	0.21	
	2,4-Decadienal	152	81	1.06	1.07	
	Decanal	156	43	2.15	2.15	
	9-Octadecenal	266	41	11.78	13.11	
Ketones	1-Methyl-bicycloheptan-6-one	124	67	5.08	5.13	
	2-Nonanone	142	43	0.14	0.14	
	Campherenone	220	41	0.05	0.06	
Sterols	Ergosterol	396	69	0.45	0.47	
	$\beta$ -Sitosterol	414	41	0.39	0.41	
	Total hydrocarbons			41.21	42.79	
	Total fatty alcohols			23	24.87	
	Total aldehydes			18.21	19.78	
	Total ketones			5.27	5.33	
	Total sterols			0.84	0.88	
	Total identified compounds			88.53	93.65	

BP, Base Peak

Table 2. HPLC Analysis of the Phenolics and Flavonoids in Ethanolic and Aqueous *C. tiglium* L. seeds Extracts before and after Incorporating ZnO-NPs.

Compound		Concentration ( $\mu\text{g/g}$ )			
		Ethanolic extract		Aqueous extract	
		Before	After	Before	After
Phenolics	Gallic acid	32.715	35.278	27.214	29.716
	Protocatechuic acid	59.866	61.425	32.086	32.981
	p-Hydroxybenzoic acid	52.587	54.842	27.264	28.094
	Gentisic acid	77.349	81.028	99.581	99.984
	Catechin	315.404	401.273	69.793	71.428
	Chlorogenic acid	94.764	101.254	112.869	117.352
	Caffeic acid	50.341	51.753	17.104	20.587
	Syringic acid	8.979	9.015	15.889	16.102
	Vanillic acid	151.947	156.284	8.171	8.987
	Ferulic acid	22.473	24.897	36.934	37.891
	Sinapic acid	11.429	18.349	0.000	0.000
	p-coumaric acid	13.241	19.257	0.000	0.000
	Rosmarinic acid	9.427	11.025	0.000	0.000
	Cinnamic acid	8.869	10.266	15.29	18.301
	Flavonoids	Quercetin	27.482	32.487	26.908
Kaempferol		34.172	36.981	29.941	33.427
Rutin		41.625	43.289	39.233	47.814
Chrysin		27.362	29.476	12.406	19.452

H-6 $\delta$ ), 5.00 (H-1 $\delta$ ).  $^{13}\text{C-NMR}$  (125 MHz, DMSO,  $\delta$ ): 157.53 (C-2), 127.48 (C-3), 180.73 (C-4), 162.14 (C-5), 93.67 (C-6), 161.43 (C-7), 93.76 (C-8), 160.45 (C-9), 99.50 (C-10), 121.47 (C-1 $\delta$ ), 103.94 (C-2 $\delta$ ), 144.25 (C-3 $\delta$ ), 154.33 (C-4 $\delta$ ), 101.43 (C-5 $\delta$ ), 114.93 (C-6 $\delta$ ), 100.00 (C-1 $\delta$ ), 72.85 (C-2 $\delta$ ), 75.64 (C-3 $\delta$ ), 63.80 (C-4 $\delta$ ), 75.21 (C-5 $\delta$ ), 60.25 (C-6 $\delta$ ).

13-O-Acetylphorbol-20-(9Z,12Z-octadecadienoate) was identified at Rf value 0.41 in  $\text{CHCl}_3$  : MeOH (70:30 v/v) and isolated as amorphous powder. UV  $\lambda_{\text{max}}$  was 245 nm; FT-IR bands at 3390  $\text{cm}^{-1}$  for stretching, 1,720  $\text{cm}^{-1}$  for C=O stretching, 1695  $\text{cm}^{-1}$  for ester linkage, 1,630  $\text{cm}^{-1}$  for -C=C- stretch. EI-MS 70 eV m/z (rel. int.): 669 (25) calculated for molecular formula  $\text{C}_{40}\text{H}_{61}\text{O}_8$ , 632 (31) [M-2H $_2$ O] $^+$ , 590 (37) [M-H $_2$ O-CH $_3$ COOH] $^+$ , and

388 (28) [M-linoleic acid] $^+$ . 13-O-Tigloylphorbol-20-(9Z,12Z-octadecadienoate) was identified at Rf value 0.46 in  $\text{CHCl}_3$ :MeOH (70:30) and isolated as amorphous powder. UV  $\lambda_{\text{max}}$  was 241 nm; FT-IR bands at 3,420  $\text{cm}^{-1}$  for stretching, 1,715  $\text{cm}^{-1}$  for C=O stretching, 1,700  $\text{cm}^{-1}$  for ester linkage, 1,625  $\text{cm}^{-1}$  for -C=C- stretch. EI-MS 70 eV m/z (rel. int.): 709 (17) calculated for molecular formula  $\text{C}_{43}\text{H}_{65}\text{O}_8$ , 590 (29) [M-tiglic acid-H $_2$ O] $^+$ , 410 (34) [M-linoleic acid] $^+$  and 328 (21) [M-tiglic acid-linoleic acid-H $_2$ O] $^+$ .

#### The structural properties of prepared ZnO-NPs

The UV-Visible spectroscopy was used for studying the optical properties of the synthesized ZnO-NPs. Data presented in Figure 1a showed that preparation of

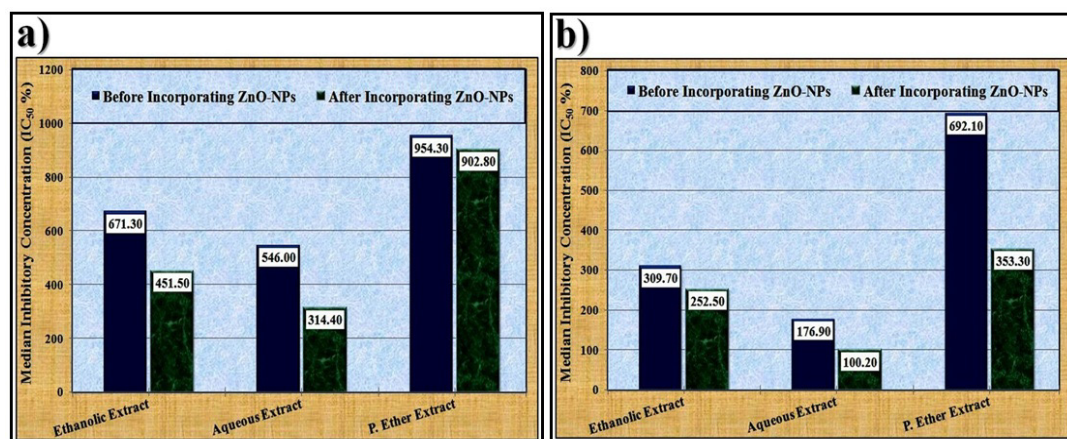


Figure 3. Cytotoxic Activity of the Different *C. tiglium* L. seeds Extracts before and after Incorporating ZnO-NPs against a) human liver cancer (HEPG-2) and b) human colon cancer (CACO-2)

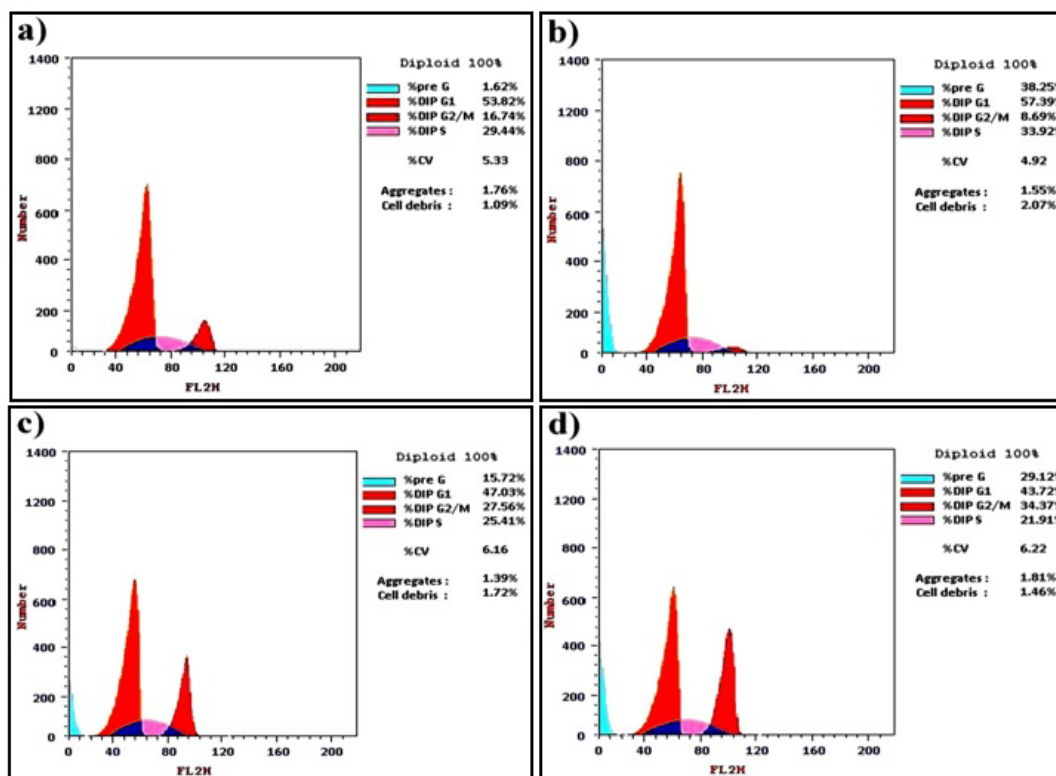


Figure 4. Data of DNA Content in a) Control CACO-2, b) CACO-2 treated with doxorubicin, c) CACO-2 treated with aqueous *C. tigrillum* L. extract and d) CACO-2 treated with ZnO-Aqueous nano-extract

ZnO-NPs from the biosynthesis route was confirmed from the sharp peak identified in the UV-visible spectrum at 382 nm. Data of the XRD pattern illustrated in Figure 1b and showed that peaks identified at  $2\theta = 31.7, 34.4, 36.2, 47.5, 56.5, 62.7, 67.8$  and  $68.1$  and assigned to (100), (002), (101), (102), (110), (103), (112) and (201)

confirmed formation of ZnO-NPs with high quality. The TEM data were in compatible to the UV and XRD data. The TEM analysis was utilized for revealing size and the crystalline characteristics of the biosynthesized ZnO-NPs. As revealed in Figure 1c, the TEM image confirmed synthesis of ZnO-NPs with morphological shape and

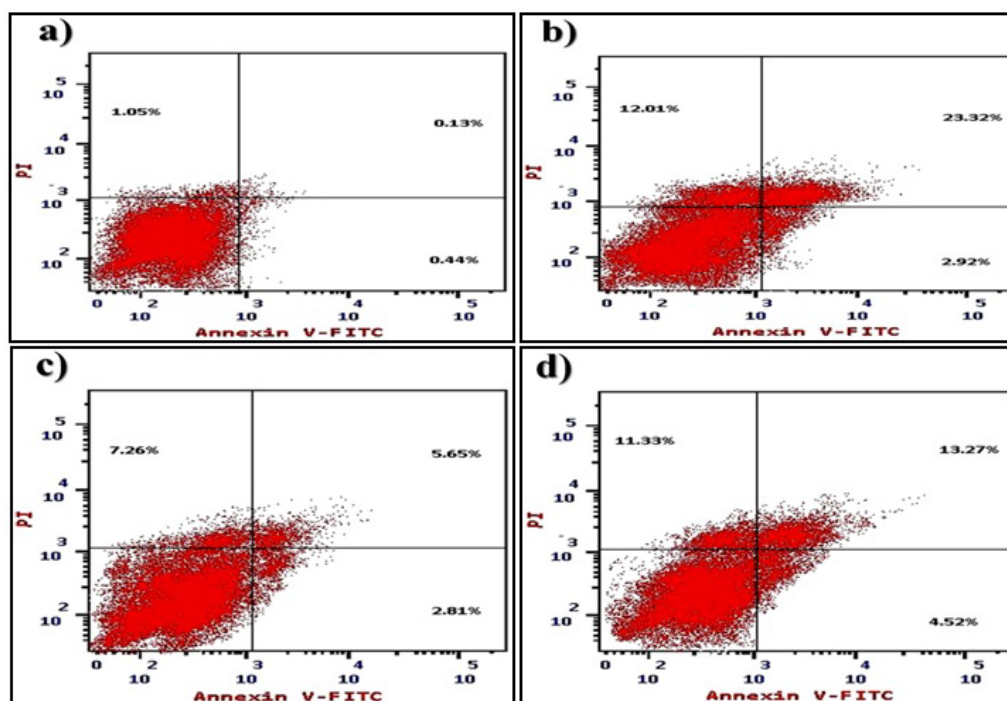


Figure 5. Data of Apoptosis Assay with Annexin V-FITC showing a) Control CACO-2, b) CACO-2 treated with doxorubicin, c) CACO-2 treated with aqueous *C. tigrillum* L. extract and d) CACO-2 treated with ZnO-Aqueous nano-extract.

Table 3. Antioxidant Activity of the Different Extracts of *C. tiglium* L. seeds before and after Incorporating ZnO-NPs

Extract	Total Polyphenols (mg gallic acid/100 gm)	Total Condensed Tannins ( $\mu\text{g/mL}$ )	Total Antioxidant Capacity (mg gallic acid/gm)	Iron Reducing Power ( $\mu\text{g/mL}$ )
Before	Ethanollic	60.02 $\pm$ 1.37	22.10 $\pm$ 0.18	103.79 $\pm$ 1.37
	Aqueous	124.44 $\pm$ 2.19*	26.95 $\pm$ 0.12*	140.53 $\pm$ 2.00*
	P. Ether	22.71 $\pm$ 1.03	-	75.76 $\pm$ 1.65
After	ZnO-Ethanollic	114.04 $\pm$ 2.61	31.13 $\pm$ 0.09	185.78 $\pm$ 2.44
	ZnO-Aqueous	236.44 $\pm$ 4.16*	36.93 $\pm$ 0.10*	251.55 $\pm$ 3.59*
	ZnO-P. Ether	43.15 $\pm$ 1.96	-	135.61 $\pm$ 2.96

\* denotes the most effective extract, Values expressed as mean of three replicates  $\pm$  SE.



Figure 6. The Median Lethal Doses ( $LD_{50}$ ) of the Different *C. tiglium* L. seeds Extracts before and after Incorporating ZnO-NPs.”

hexagonal polycrystalline structure with approximately size ranged from 20 to 70 nm. The catalytic activity of the synthesized ZnO-NPs is strongly related to their hexagonal structure that implies more ionicity. The ZnO-NPs are well dispersed and some of them are irregular in their shapes. Furthermore, it was emphasized that the particles are almost spherical with a slight variation in thickness. The particle size that was determined by TEM technique is almost close to that obtained by XRD analysis. DLS is an accurate procedure to use a monodisperse dilute solution for measuring particle size ranged from 5 nm to 5  $\mu\text{m}$ . Data of the DLS illustrated in Figure 1d, showed that the particle size distribution and the hydrodynamic size of the

fabricated ZnO-NPs has main diameter around 164 nm.

#### *The phyto-constituents in C. tiglium* L. seeds extracts before and after incorporating ZnO-NPs

Data of GC/MS analysis of petroleum ether *C. tiglium* L. extract depicted in Table 1 showed that 38 compounds representing 88.53% were identified; where the identified lipoidal components consist of 17 hydrocarbons (41.21%), 9 fatty alcohols (23.0%), 7 aldehydes (18.21%), 3 ketones (5.27%) and 2 sterols (0.84%). It was found that n-octadecane, hentriacontane and tetracosane were the major identified hydrocarbons in petroleum ether extract representing 5.61, 7.04 and

Table 4. The 1,1-diphenyl-2-picrylhydrazyl (DPPH) and 2,2'-azinobis-(3-ethylbenzothiazoline-6-sulfonic acid) (ABTS) Radicals Scavenging Activity of the Different Extracts of *C. tiglium* L. seeds before and after Incorporating ZnO-NPs

Extract	$IC_{50}$ ( $\mu\text{g/mL}$ )	Inhibition of ABTS Radicals (%)
Before	Ethanollic	18.92 $\pm$ 0.05
	Aqueous	12.91 $\pm$ 0.11*
	P. Ether	28.89 $\pm$ 0.06
After	ZnO-Ethanollic	7.17 $\pm$ 0.03
	ZnO-Aqueous	3.78 $\pm$ 0.02*
	ZnO-P. Ether	11.23 $\pm$ 0.04
Ascorbic acid (Standard)	3.83 $\pm$ 0.02	36.78 $\pm$ 0.03

\* denotes the most effective extract, Values expressed as mean of three replicates  $\pm$  SE.

Table 5. Anti-Arthritic Activity of the Different *C. tiglium* L. seeds Extracts before and after Incorporating ZnO-NPs

Extract		Proteinase Denaturation (%)	Inhibition of Proteinase Activity (%)
Before	Ethanollic	36.99 ± 0.48	31.91 ± 0.66
	Aqueous	52.44 ± 0.67*	52.22 ± 0.42*
	P. Ether	26.19 ± 0.66	32.28 ± 0.60
After	ZnO-Ethanollic	67.77 ± 0.39	52.46 ± 0.66
	ZnO-Aqueous	78.99 ± 0.44*	75.17 ± 0.99*
	ZnO-P. Ether	45.65 ± 1.11	46.75 ± 0.65
Diclofenac sodium (Standard)		48.68 ± 0.24	40.46 ± 0.73

\* denotes the most effective extract, Values expressed as mean of three replicates ± SE.

Table 6. Cytotoxic Activity of the Different *C. tiglium* L. Seeds Extracts against Human Liver (HEPG-2) and Colon Cancer (CACO-2) Cells before and after Incorporating ZnO-NPs.

Extract		IC <sub>50</sub> %	
		HEPG-2	CACO-2
Before	Ethanollic	671.3	309.70
	Aqueous	546.00*	176.90*
	P. Ether	954.3	692.10
After	ZnO-Ethanollic	451.5	252.50
	ZnO-Aqueous	314.40*	100.20*
	ZnO-P. Ether	902.8	353.30

\* denotes the most effective extract, Values expressed as mean of three replicates ± SE.

6.54%, respectively. While 2-nonen-1-ol (12.25%) was considered as the main identified fatty alcohol. In addition, 9-octadecenal and 1-methyl-bicycloheptan-6-one are the most common aldehydic and ketonic compounds with the highest concentration representing 11.78 and 5.08%, respectively. Beside to identification of 2 steroidal compounds ergosterol and  $\beta$ -sitosterol representing 0.45 and 10.39%, respectively.

It was worthy to mention that the phyto-constituents identified in petroleum ether extract were not changed or missed after incorporating ZnO-NPs, but their values increased. It was noticed that concentration of the total hydrocarbons in that extract elevated from 41.21 to 42.79%, total fatty alcohols increased from 23.0 to 24.87%. Additionally, the total aldehydes and ketones concentration raised from 18.21 to 19.78%, and

Table 7. Data of the EGFR, Bcl2 and Casp3 Genes Expression in Human Colon Cancer (CACO-2) Cells Treated with Aqueous *C. tiglium* L. extract before and after Incorporating ZnO-NPs

Extract	Conc. ( $\mu$ M)	EGFR							FLD 2 <sup>-<math>\Delta\Delta</math>CT</sup> Eamp=1.849
		Control cells			Test cells				
		GAPDH HC	EGFR TC	$\Delta$ CTC TC-HC	GAPDH HE	EGFR TE	$\Delta$ CTE TE-HE	$\Delta\Delta$ CT $\Delta$ CTE- $\Delta$ CTC	
Aqueous <i>C. tiglium</i> extract	23.46	26.82	3.36	24.08	27.86	3.78	0.42	0.77	
ZnO-Aqueous nano-extract	23.46	26.82	3.36	23.82	28.55	4.73	1.37	0.43	
Doxorubicin	23.46	26.82	3.36	23.91	29.21	5.3	1.94	0.30	
Control	23.46	26.82	3.36	23.46	26.82	3.36	0.00	1.00	

Extract	Conc. ( $\mu$ M)	Bcl2							FLD 2 <sup>-<math>\Delta\Delta</math>CT</sup> Eamp=1.849
		Control cells			Test cells				
		GAPDH HC	Bcl2 TC	$\Delta$ CTC TC-HC	GAPDH HE	Bcl2 TE	$\Delta$ CTE TE-HE	$\Delta\Delta$ CT $\Delta$ CTE- $\Delta$ CTC	
Aqueous <i>C. tiglium</i> extract	23.46	28.76	5.30	24.08	30.15	6.07	0.77	0.62	
ZnO-Aqueous nano-extract	23.46	28.76	5.30	23.82	30.58	6.76	1.46	0.41	
Doxorubicin	23.46	28.76	5.30	23.91	30.83	6.92	1.62	0.37	
Control	23.46	28.76	5.30	23.46	28.76	5.30	0.00	1.00	

Extract	Conc. ( $\mu$ M)	Casp3							FLD 2 <sup>-<math>\Delta\Delta</math>CT</sup> Eamp=1.849
		Control cells			Test cells				
		GAPDH HC	Casp3 TC	$\Delta$ CTC TC-HC	GAPDH HE	Casp3 TE	$\Delta$ CTE TE-HE	$\Delta\Delta$ CT $\Delta$ CTE- $\Delta$ CTC	
Aqueous <i>C. tiglium</i> extract	23.46	33.61	10.20	24.08	32.75	8.67	-1.48	2.48	
ZnO-Aqueous nano-extract	23.46	33.61	10.20	23.82	31.62	7.80	-2.35	4.24	
Doxorubicin	23.46	33.61	10.20	23.91	30.79	6.88	-3.27	7.46	
Control	23.46	33.61	10.20	23.46	33.61	10.2	0.00	1.00	

from 5.27 to 5.33%, respectively. Beside to increasing concentration of sterols content from 0.84 to 0.88%. Increasing concentration of the lipoidal components was responsible for improving the biological activities by synergetic mechanism between all compounds of the petroleum ether extract.

Data of HPLC analysis compiled in Table 2 showed that the phenolic compounds that were identified in the ethanolic and aqueous *C. tiglium* L. seeds extracts were about 14 and 11, respectively. Moreover, 4 flavonoidal compounds were noticed in both ethanolic and aqueous extracts. It was noticed that catechin and vanillic acid were the most predominant phenolic compounds identified in the ethanolic *C. tiglium* L. extract and their concentration increased from 315.404 and 151.947  $\mu\text{g/g}$  to 401.273 and 156.284  $\mu\text{g/g}$ , respectively after incorporating ZnO-NPs. As regard to the aqueous *C. tiglium* L. extract, gentisic acid and chlorogenic acid were considered as the most common phenolic compounds and their concentrations increased from 99.581 and 112.869  $\mu\text{g/g}$  to 99.984 and 117.352  $\mu\text{g/g}$ , respectively after incorporating ZnO-NPs. On the other hand, rutin was identified as the major flavonoidal compound in both ethanolic and aqueous *C. tiglium* L. seeds extracts. Its concentration increased from 41.625 and 39.233  $\mu\text{g/g}$  to 43.289 and 47.814  $\mu\text{g/g}$ , respectively after incorporating ZnO-NPs.

In vitro study on different *C. tiglium* L. seeds extracts before and after incorporating zinc oxide nanoparticles

As presented in Table 3, total polyphenolic compounds and condensed tannins are the major active phyto-constituents in the different *C. tiglium* L. seeds extracts. The aqueous *C. tiglium* L. seeds extract contains the highest concentration of total polyphenolic compounds (124.44  $\pm$  2.19 mg gallic acid/100 gm) and condensed tannins (26.95  $\pm$  0.12  $\mu\text{g/mL}$ ) more than the other *C. tiglium* L. extracts. Incorporation of ZnO-NPs into the aqueous *C. tiglium* L. seeds extract increased concentrations of total polyphenolic compounds and condensed tannins to 236.44  $\pm$  4.16 mg gallic acid/100 gm and 36.93  $\pm$  0.10  $\mu\text{g/mL}$ , respectively.

The biological activities of the different *C. tiglium* L. seeds extracts were assayed by measuring the total antioxidant capacity and iron reducing power in addition to the scavenging activity against DPPH and ABTS radicals using ascorbic acid as standard. The total antioxidant capacity and iron reducing power are closely related to concentrations of the total polyphenols and total condensed tannins. Therefore, it was noticed that the aqueous *C. tiglium* L. seeds extract exhibited the highest the antioxidant activity (140.53  $\pm$  2.00 mg gallic acid/gm) and iron reducing power (138.82  $\pm$  4.51  $\mu\text{g/mL}$ ) as illustrated in Table 3. Incorporation of ZnO-NPs into the aqueous *C. tiglium* L. seeds extract increased the antioxidant activity and iron reducing power to 251.55  $\pm$  3.59 mg gallic acid/gm and 249.88  $\pm$  8.12  $\mu\text{g/mL}$ , respectively.

As regard to the scavenging activity against DPPH and ABTS radicals, it was found that the aqueous *C. tiglium* L. seeds extract possessed the highest scavenging activity. Strong scavenging activity against DPPH radical was indicated by low  $\text{IC}_{50}$  value. As presented in Table 4,

the lowest  $\text{IC}_{50}$  value (12.91  $\pm$  0.11  $\mu\text{g/mL}$ ) was noticed with the aqueous *C. tiglium* L. seeds extract as compared to the other extracts. Moreover, it showed the highest scavenging activity against ABTS radical (41.11  $\pm$  0.07%) at equal concentrations of all studied extracts, whereas at the same concentration, the standard ascorbic acid was 36.78  $\pm$  0.03%. Incorporation of ZnO-NPs into the aqueous *C. tiglium* L. seeds extract increased the scavenging activity by lowering the  $\text{IC}_{50}$  value required to inhibit DPPH radical to 3.78  $\pm$  0.02  $\mu\text{g/mL}$  and increasing inhibition of ABTS radical to 62.91  $\pm$  0.10%.

As revealed in Figure 2a, it was found that the aqueous *C. tiglium* L. seeds extract exhibited the highest inhibitory effect at equal concentrations on  $\alpha$ -amylase and AChE activities (41.89 and 23.00%, respectively). Incorporating ZnO-NPs into the aqueous extract increased their inhibitory effect against  $\alpha$ -amylase and AChE activities to 67.97 and 49.91%, respectively (Figure 2b).

Data depicted in Table 5 showed percentage of protein denaturation and proteinase inhibitory activity. It was noticed that the aqueous *C. tiglium* L. seeds extract showed higher protein denaturation (52.44  $\pm$  0.67%) and proteinase inhibitory activity (52.22  $\pm$  0.42%) compared to diclofenac sodium that was used as a powerful non-steroidal anti-inflammatory standard drug. Incorporation of ZnO-NPs into the aqueous extract showed better protein denaturation (78.99  $\pm$  0.44%) and proteinase inhibitory activity (75.17  $\pm$  0.99%) than the reference drug (diclofenac sodium) and the native aqueous extract itself.

Data compiled in Table 6 and illustrated in Figure 3a showed that the aqueous *C. tiglium* L. seeds extract exhibited the highest cytotoxic activity ( $\text{IC}_{50}$  546.00  $\mu\text{g/mL}$ ) against HEPG-2 cells compared to the other native extracts. The Supplementary 1 showed the maximum (Conc. 1,000  $\mu\text{g/mL}$ ) and  $\text{IC}_{50}$  of different native *C. tiglium* L. seeds extracts compared to control HEPG-2 cells. It was found that incorporation of ZnO-NPs into aqueous extract increased the cytotoxic activity against HEPG-2 cells compared to native aqueous extract itself ( $\text{IC}_{50}$  314.40  $\mu\text{g/mL}$ ). The Supplementary 2 showed the maximum (Conc. 1000  $\mu\text{g/mL}$ ) and  $\text{IC}_{50}$  of different *C. tiglium* L. seeds extracts after incorporating ZnO-NPs compared to control HEPG-2 cells. As regard to the in vitro cytotoxic activity against CACO-2, data depicted in Table 6 and illustrated in Figure 3b showed that the aqueous *C. tiglium* L. seeds extract exhibited the highest cytotoxic activity ( $\text{IC}_{50}$  176.90  $\mu\text{g/mL}$ ) against CACO-2 cells compared to the other native extracts. The Supplementary 3 showed the maximum (Conc. 1,000  $\mu\text{g/mL}$ ) and  $\text{IC}_{50}$  of different native *C. tiglium* L. seeds extracts compared to control CACO-2 cells. Incorporation of ZnO-NPs into aqueous extract elevated the cytotoxic activity against CACO-2 cells compared to native aqueous extract itself ( $\text{IC}_{50}$  100.20  $\mu\text{g/mL}$ ). The Supplementary 4 showed the maximum (Conc. 1000  $\mu\text{g/mL}$ ) and  $\text{IC}_{50}$  of different *C. tiglium* L. seeds extracts after incorporating ZnO-NPs compared to control CACO-2 cells. In the present study, it was found that the cytotoxic activity of the aqueous *C. tiglium* L. seeds extract increased after incorporating ZnO-NPs

As revealed in Supplementary 5, it was found that treatment of CACO-2 cells with the aqueous *C. tiglium*

L. seeds extract incorporated with ZnO-NPs decreased the fold changes of EGFR and Bcl2 genes (0.43 and 0.41, respectively) compared to the native aqueous extract itself (0.77 and 0.62, respectively). As regard to Casp3 gene, the aqueous *C. tiglium* L. seeds extract incorporated with ZnO-NPs increased its fold changes (4.24) more than the native aqueous extract itself (2.48). Treatment of CACO-2 cells with the native aqueous *C. tiglium* L. seeds extract or the aqueous extract incorporated with ZnO-NPs arrested the cell growth at G2/M compared to doxorubicin that arrested the cell growth at G1/S (Supplementary 6). As illustrated in Supplementary 7, treatment of CACO-2 cells with the aqueous *C. tiglium* L. seeds extract incorporated with ZnO-NPs increased percentage of the total apoptotic cells (29.12%) and increased percentage of the early (4.52%) and late apoptotic cells (13.27%) as compared to control CACO-2 or those cells treated with the native aqueous extract itself. Moreover, percentage of the necrosis increased in the CACO-2 cells treated with ZnO-aqueous nano-extract (11.33%) more than those cells treated with the native aqueous extract (7.26%). Data presented in Table 7 showed that incorporation of ZnO-NPs into the aqueous *C. tiglium* L. seeds extract caused on significant changes in expression of the EGFR, Bcl2 and Casp3 genes in the treated CACO-2 cells as compared to control HEPG-2 or those cells treated with the native extract itself.

Data of the flow cytometric analysis presented in Figure 4 and using Annexin V-FITC as shown in Figure 5 showed that treatment of CACO-2 cells with the native aqueous *C. tiglium* seeds extract or the aqueous extract incorporated with ZnO-NPs enhanced apoptosis as compared to control CACO-2 cells.

#### *Toxicity of different C. tiglium L. seeds extracts before and after incorporating ZnO-NPs*

It was noticed that the LD<sub>50</sub> values of ethanolic, aqueous and P. ether extracts were about 7667, 8083 and 5500 mg/Kg, respectively. After incorporating ZnO-NPs, the LD<sub>50</sub> values increased to 11000, 11333 and 9500 mg/Kg, respectively (Figure 6).

## Discussion

#### *The nutritional composition of C. tiglium L. seeds*

During the current study, it was noticed that *C. tiglium* L. seeds provided great values and could be consumed for either nutritional or medicinal purposes which in agreement with Owade et al. (2019) and supported by Aboulthana et al. (2019) who stated that *C. tiglium* L. seeds have been utilized mainly for its oil, protein and polysaccharide contents.

#### *The major compounds isolation from different C. tiglium L. seeds extracts*

During the present study, the steroidal ( $\beta$ -sitosterol and stigmasterol) and the pentacyclic triterpenoid ( $\alpha$ -amyrin) compounds were identified and isolated in pure form and this was in agreement with the study carried out by Smina et al. (2011). Their spectroscopical data were in agreement with that reported by El-Feky et al. (2018). Furthermore,

isopimara-7,15-dien-3 $\beta$ -ol is diterpene compound isolated from leaves of *Croton zambesicus* by Block et al. (2004) and not identified before from *C. tiglium* L. seeds. Although numerous quercetin derivatives were identified by Guerrero et al. (2002) from *Croton schiedeanus* L., quercetin-7-O- $\beta$ -D-glucopyranoside was isolated and identified for the first time from *C. tiglium* L. seeds during the present study. In the current experiment, 13-O-Acetylphorbol-20-(9Z,12Z-octadecadienoate) and 13-O-Tigloylphorbol-20-(9Z,12Z-octadecadienoate) were isolated and identified. These two phorbol esters were previously isolated from *C. tiglium* L. seeds by El-Mekkawy et al., (2000).

#### *The structural properties of prepared ZnO-NPs*

The biosynthesized ZnO-NPs was identified as sharp peak identified in the UV-visible spectrum at 382 nm and this agreed with the experiment carried out by Kavitha et al. (2013) who reported that the peak at 280 nm corresponds to the plant extract. Moreover, the strong absorption band that was assigned to the intrinsic band-gap absorption of ZnO might be attributable to transition of the electron from the valence to conduction band (Khorsand Zak et al., 2013). The DLS showed that the zeta potential denotes repulsion degree between adjacent particles (with similar charges) in dispersions (Hassan et al., 2019). Moreover, the particle size distribution and the hydrodynamic size of the fabricated ZnO-NPs has main diameter around 164 nm. This agreed with Kim et al. (2012) who reported that the synthesized ZnO-NPs can form aggregates (lumps of primary particles held together by strong chemical bonds) or agglomerates (groups of primary particles gathered by weak van der Waals forces) in a liquid dispersion of dry powder.

#### *In vitro study on different C. tiglium L. seeds extracts before and after incorporating ZnO-NPs*

Due to the presence of various active bio-components like alkaloids, terpenoids, phenolics, tannins, saponins, polysaccharides, proteins, enzymes and vitamins, plant extract can be used as a potential substitute for reducing agents (Ahmed et al., 2016). It was found that the aqueous *C. tiglium* L. seeds extract is in the highest concentrations of total polyphenolic compounds and condensed tannins more than the other *C. tiglium* L. extracts. The phenolic compounds and flavonoids are secondary metabolites exist in almost all medicinal plants. Antioxidative and anti-carcinogenic activities are considered as the most common biological activities of these phyto-constituents in addition to their role as bio-reductants of metallic ions in aqueous medium (Yuvakkumar et al., 2014). This might be attributed to the presence of the functional groups responsible for the bio-reduction and stabilization process during biosynthesis of metal and metal oxide NPs (XiuLan et al., 2017). During the ZnO-NPs biosynthesis, phenol and flavonoids in plant extract react with zinc nitrate by binding zinc surface to control the particle size after activating the ZnO-NPs biosynthesis. These phyto-constituents are responsible for reducing and capping activity due to existence of a large number of OH groups (Bala et al., 2015).

It was noticed that aqueous *C. tiglium* L. seeds extract exhibited the highest the antioxidant activity and this might be attributed to the complex nature of the phenolic compounds and the other phytochemicals that have redox properties enable them to act as hydrogen donors and hence to be used as reducing agents. The plant extracts possessed higher scavenging activities against the oxidative stress induced by Reactive Oxygen (ROS) and Nitrogen Species (RNS) due to the presence of these active constituents with high concentrations as suggested by Kalim and Nikalje (2017).

DPPH and ABTS free radical scavenging assays provide an easy and rapid methods for estimating ability of the antioxidants to scavenge free radical based on quenching stable-colored radicals (Zia-UI-Haq et al., 2012). During the current study, it was noticed that the scavenging activity of the extract incorporated with ZnO-NPs increased and this was confirmed by decreasing the absorbance at 517 nm as a result of changing color of the reaction product from purple to yellow. This agreed with Nagajyothi et al. (2015) who emphasized that the antioxidant activity of the extract increased after incorporating ZnO-NPs due to presence of the active phyto-constituents that were responsible for imparting antioxidant capabilities and utilized throughout manufacturing of ZnO-NPs for their reduction and stabilization.

$\alpha$ -amylase is the most essential digestive tract enzyme required for hydrolyzing carbohydrates. Therefore, inhibition of this enzyme is one of the most suitable ways for lowering postprandial hyperglycemia (Nair et al., 2013). Moreover, AChE enzyme exhibits its role in tissue synapses or neuromuscular junctions through catalyzing the hydrolysis process during which acetyl choline (a neurotransmitter) is converted into choline and acetic acid. Therefore, activation of this enzyme is one of leading cause of Alzheimer's disease. Inhibition of this enzyme is one of the suitable ways necessary for Alzheimer treatment (Suganthi et al., 2018). It was found that incorporation of ZnO-NPs into the aqueous extract increased their inhibitory effect against  $\alpha$ -amylase and AChE activities and this agreed with Jan et al., (2021) who emphasized that existence of ZnO-NPs in aqueous *C. tiglium* L. seeds extract showed higher anti-diabetic properties through suppressing  $\alpha$ -amylase activity. This might be attributed . The biosynthesized ZnO-NPs exhibited efficient anti-Alzheimer's activity by inhibiting AChE activity and this agreed with Khalil et al. (2019) who reported that ZnO-NPs belongs to the M-NPs that suppressed AChE followed by cobalt oxide and iron oxide nanoparticles.

Inflammation is a response process by which living tissues react towards injury. It is considered as the most common phenomenon that occurs during arthritis and induced by denaturation of protein. Inflammation and activity of immune response decreased by steroids (Nagajyothi et al., 2014). It was found that the aqueous *C. tiglium* L. seeds extract showed higher protein denaturation and proteinase inhibitory activity. Incorporation of ZnO-NPs into the aqueous extract showed better protein denaturation and proteinase inhibitory activity than the native aqueous extract itself.

This agreed with Senthilkumar et al. (2017) who revealed that the presence of ZnO-NPs enhanced the anti-arthritis activity of the extract due to their capability for inhibiting protein denaturation and proteinase inhibitory activity. This might be related to increasing the scavenging activity against the free radicals that are critically involved in arthritis and inflammation.

Cell viability assays are considered as basic criteria to reveal the cellular response to toxic substances and to elucidate efficiency of the extract against incidence and progression of cancer cells by the MTT assay. A calcein (green fluorescent compound) that produced from calcein AM as a result of role of active esterase exists with intact membranes in living cells serves as a marker for viable cells. Moreover, there is red fluorescent nucleic acid stain called propidium iodide (PI) used for detecting the damaged cells that take up the dye and stain positive and it has no the ability to penetrate normal cells (Sanlioglu et al., 2007). Studying efficiency of the anti-cancer potential of ZnO-NPs against growth and progression of cancer cells belongs to scientific hotspots for cancer therapy (Vimala et al., 2014). During the current study, the in vitro cytotoxicity of different *C. tiglium* L. seeds extracts was studied after incorporating ZnO-NPs against HEPG-2 and CACO-2 in comparison with native extracts.

Data of the current study showed that the cytotoxic activity of the aqueous *C. tiglium* L. seeds extract increased after incorporating ZnO-NPs and this agreed with the study carried out by Modena et al. (2019) who emphasized that the cytotoxic activity might be attributed to presence of alcohols and phenolic groups in addition to C-N stretching vibrations of aromatic amines of biomolecules on the surface of the biosynthesized ZnO-NPs that physiologically act on inhibiting growth of cancer cells. Furthermore, the plant-derived ZnO-NPs showed an exciting potential as promising anti-cancer agents by enhancing the cellular death through production of the ROS that disrupt signal transduction pathways (Ismail et al., 2018). When ZnO-NPs get entry into the cancerous cell, they produced ROS species, disturbed depolarization of the membrane and damaged DNA; all these events eventually leads to apoptosis or death of cancer cell (Jan et al., 2020). During the current study, it was noticed that the aqueous *C. tiglium* L. seeds extract showed better cytotoxic activity against CACO-2 than HEPG-2 cells. Therefore, it was selected for undergoing further studies on CACO-2 cells before and after incorporating ZnO-NPs.

Data of the flow cytometric analysis showed that treatment of CACO-2 cells with the native aqueous *C. tiglium* seeds extract or the extract incorporated with ZnO-NPs enhanced apoptosis as compared to control CACO-2 cells. This agreed with Jan et al., (2021) who postulated that ZnO-NPs showed prominent apoptosis after for 24 h treatment. The cytotoxic activity of ZnO-NPs against growth and progression of human cancer cells occurred through three primary mechanisms including breakdown of the ZnO-NPs into Zn<sup>2+</sup>, ROS production and DNA damage. In addition, the physical properties (size, surface chemistry and dose) of the ZnO-NPs dictate their overall uptake, elimination and antitumor

properties (Chen et al., 2019). Also, ZnO-NPs have the ability to induce apoptosis in CACO-2 cells by oxidative stress leading to cytotoxicity, inflammatory responses, mitochondrial membrane alterations and release of interleukin-8 in cancerous cells (Jain et al., 2018). It was demonstrated that ZnO-NPs showed their anticancer and antiproliferative effect via up-regulating the apoptotic and tumor suppressor genes, down-regulating the antiapoptotic genes, inducing ROS production, DNA fragmentation and caspase-3 enzyme in cancer cells (Ismail et al., 2014 ; Iswarya et al., 2017).

#### *Toxicity of different C. tiglium L. seeds extracts before and after incorporating ZnO-NPs*

It was found that administration of the different *C. tiglium L.* seeds extracts incorporated with ZnO-NPs orally was safer than the native extracts. This was agreement with Shaban et al., (2021) and supported recently by Aboulthana et al., (2022) who reported that no significant alterations detected in the biochemical markers after oral administration of M-NPs. Biodistribution of the M-NPs in organs and tissues depends highly on size and dose of the M-NPs. Size of the M-NPs is considered as the most important factor affecting their biodistribution. Ratio of the large surface area to volume of the NPs stimulates their interactions with the macromolecules in biological systems (Wang et al., 2020). Biosynthesis of M-NPs by mean of green nanotechnology found with less toxicity and it increased safety of plant extract in which the M-NPs incorporated (Abdel-Halim et al., 2020). This was attributed to efficiency the renal tissue to eliminate the M-NPs with low degradation rate in the body to avoid the undesirable side effects (Aboulthana et al., 2019).

#### **Author Contribution Statement**

Wael M. Aboulthana: Writing – original draft, Writing – review & editing, Visualization, Supervision and Project administration. Nagwa I. Omar: Resources, Data curation, Writing – review & editing. Amal M. El-Feky: Methodology, Validation, Formal analysis, Writing – review & editing. Enas A. Hasan: Formal analysis, Writing – review & editing. Noha E. Ibrahim: Literature collection, Writing – review & editing. Ahmed M. Youssef: Conceptualization, Data curation, Writing – review & editing. All authors have read and agreed to the published version of the manuscript.

#### **Acknowledgments**

This research was accomplished in laboratories of the National Research Centre, Dokki, Giza, Egypt and provided by researchers of different scientific fields.

#### *Ethical statement*

Handling of the animals and the experimental design were carried out based on the guidelines reported in “Guide for the care and use of laboratory animal” and according to the protocol that approved by Institutional Animal Ethical Committee of National Research Centre, Dokki, Giza, Egypt.

#### *Conflict of interest*

The authors declare that they have no known competing financial interests or personal relationships that could have appeared to influence the work reported in this paper.

#### **References**

- Abdel-Halim AH, Fyad AA, Aboulthana WM, et al (2020). Assessment of the anti-diabetic Effect of Bauhinia variegata gold nano-extract against streptozotocin induced diabetes mellitus in rats. *J Appl Pharm Sci*, **10**, 77-91.
- AboulNaser A, Younis E, El-Feky A, et al (2020). Management of Citrus sinensis peels for protection and treatment against gastric ulcer induced by ethanol in rats. *Biomarkers*, **25**, 349-59.
- Aboulthana WM, Ibrahim NE, Osman NM, et al (2020). Evaluation of the Biological Efficiency of Silver Nanoparticles Biosynthesized Using Croton tiglium L. Seeds Extract against Azoxymethane Induced Colon Cancer in Rats. *Asian Pac J Cancer Prev*, **21**, 1369-89.
- Aboulthana WM, Omar NI, Hasan EA, et al (2022). Assessment of the Biological Activities of Egyptian Purslane (*Portulaca oleracea*) Extract after Incorporating Metal Nanoparticles, in Vitro and in Vivo Study. *Asian Pac J Cancer Prev*, **23**, 287-310.
- Aboulthana WM, Youssef AM, El-Feky AM, et al (2019). Evaluation of antioxidant efficiency of Croton tiglium L. seeds extracts after incorporating silver Nanoparticles. *Egypt J Chem*, **62**, 181-200.
- Aboulthana WM, Youssef AM, Seif MM, et al (2021). Comparative Study between Croton tiglium Seeds and Moringa oleifera Leaves Extracts, after Incorporating Silver Nanoparticles, on Murine Brains. *Egypt J Chem*, **64**, 1709-31.
- Ahmed S, Ahmad M, Swami BL, et al (2016). A review on plants extract mediated synthesis of silver nanoparticles for antimicrobial applications: A green expertise. *J Adv Res*, **7**, 17-28.
- Ali K, Dwivedi S, Azam A, et al (2016). Aloe vera extract functionalized zinc oxide nanoparticles as nanoantibiotics against multi-drug resistant clinical bacterial isolates. *J Colloid Interface Sci*, **427**, 145-56.
- Arnao MB, Cano A, Acosta M (2001). The hydrophilic and lipophilic contribution to total antioxidant activity. *Food Chem*, **73**, 239-44.
- Babahmad RA, Aghraz A, Boutafda A, et al (2018). Chemical composition of essential oil of *Jatropha curcas L.* leaves and its antioxidant and antimicrobial activities. *Ind Crop Prod*, **121**, 405-10.
- Bala N, Saha S, Chakraborty M, et al (2015). Green synthesis of zinc oxide nanoparticles using Hibiscus subdariffa leaf extract: effect of temperature on synthesis, anti-bacterial activity and anti-diabetic activity. *RSC Adv*, **5**, 4993-5003.
- Bao SJ, Lei C, Xu MW, et al (2012). Environment-friendly biomimetic synthesis of TiO<sub>2</sub> nanomaterials for photocatalytic application. *Nanotechnology*, **23**, 205601.
- Block S, Baccelli C, Tinant B, et al (2004). Diterpenes from the leaves of *Croton zambesicus*. *Phytochemistry*, **65**, 1165-71.
- Broadhurst RB, Jones WT (1978). Analysis of condensed tannins using acidified vanillin. *J Sci Food Agric*, **48**, 788-94.
- Chen LQ, Fang L, Ling J, et al (2015). Nanotoxicity of silver nanoparticles to red blood cells: size dependent adsorption, uptake, and hemolytic activity. *Chem Res Toxicol*, **28**, 501-9.
- Chen P, Wang H, He M, et al (2019). Size-dependent cytotoxicity study of ZnO nanoparticles in HepG2 cells. *Ecotoxicol*

- Environ Safety*, **171**, 337-46.
- Coelho MS, Salas-Mellado MM (2014). Chemical Characterization of Chia (*Salvia hispanica* L.) for Use in Food Products. *J Food Nutr Res*, **2**, 263-9.
- Das S, Sureshkumar P (2016). Effect of methanolic root extract of *Blepharispermum subsessile* DC in controlling arthritic activity. *Res J Biotechnol*, **11**, 65-74.
- El Gendy A, Leonardi M, Mugnaini L, et al (2015). Chemical composition and antimicrobial activity of essential oil of wild and cultivated *Origanum syriacum* plants grown in Sinai, Egypt. *Ind Crop Prod*, **67**, 201-7.
- El-Feky AM, Elbatanony MM, AboulNaser AF, et al (2020). Phytoconstituents and In Vitro Anti-oxidant, Anti-viral, Anti-hyperlipidemic and Anticancer Effects of *Chlorella vulgaris* Microalga in Normal and Stress Conditions. *Der Pharma Chemica*, **12**, 9-20.
- El-Feky AM, Elbatanony MM, AboulNaser AF, et al (2018). A therapeutic insight of carbohydrate and fixed oil from *Plantago ovata* L. seeds against ketoprofen-induced hepatorenal toxicity in rats. *Bull Nat Res Centre*, **42**, 28.
- Ellman GL, Courtney KD, Andres VJ, et al (1961). A new and rapid colorimetric determination of acetylcholinesterase activity. *Biochem Pharmacol*, **7**, 88-95.
- El-Mekawy S, Meselhy MR, Nakamura N, et al (2000). Anti-HIV-1 phorbol esters from the seeds of *Croton tiglium*. *Phytochemistry*, **53**, 457-64.
- Elsawi SA, Radwan RR, Elbatanony MM, et al (2020). Prophylactic Effect of *Opuntia ficus indica* Fruit Peel Extract against Irradiation-Induced Colon Injury in Rats. *Planta Medica*, **86**, 61-9.
- El-Sayed AB, Aboulthana WM, El-Feky AM, et al (2018). Bio and Phyto-chemical Effect of *Amphora coffeaeformis* Extract against Hepatic Injury Induced by Paracetamol in Rats. *Mol Biol Rep*, **45**, 2007-23.
- Ferdous Z, Nemmar A (2020). Health impact of silver nanoparticles: a review of the biodistribution and toxicity following various routes of exposure. *Int J Mol Sci*, **21**, 2375.
- Hameed AS (2018). A new coating for non-resorbable surgical suture. *J Univ Babylon Eng Sci*, **26**, 301-7.
- Harkat-Madouri L, Asma B, Madani K, et al (2015). Chemical composition, antibacterial and antioxidant activities of essential oil of *Eucalyptus globulus* from Algeria. *Ind Crop Prod*, **78**, 148-53.
- Hassan SSM, Abdel-Shafy HI, Mansour MSM (2019). Removal of pharmaceutical compounds from urine via chemical coagulation by green synthesized ZnO-nanoparticles followed by microfiltration for safe reuse. *Arabian J Chem*, **12**, 4074-83.
- Hu J, Gao WY, Gao Y, et al (2010). M3 muscarinic receptor- and Ca<sup>2+</sup> influx-mediated muscle contractions induced by croton oil in isolated rabbit jejunum. *J Ethnopharmacol*, **129**, 377-80.
- Ismail AF, Ali MM, Ismail LF (2014). Photodynamic therapy mediated antiproliferative activity of some metal-doped ZnO nanoparticles in human liver adenocarcinoma HepG2 cells under UV irradiation. *J Photochem Photobiol B Biol*, **138**, 99-108.
- Ismail EH, Saqer A, Assirey E, et al (2018). Successful green synthesis of gold nanoparticles using a *Corchorus olitorius* extract and their antiproliferative effect in cancer cells. *Int J Mol Sci*, **19**, 2612.
- Iswarya A, Vaseeharan B, Anjugam M, et al (2017). Multipurpose efficacy of ZnO nanoparticles coated by the crustacean immune molecule  $\beta$ -1, 3-glucan binding protein: toxicity on HepG2 liver cancer cells and bacterial pathogens. *Colloids Surf B Biointerfaces*, **158**, 257-69.
- Jain A, Ranjan S, Dasgupta N, et al (2018). Nanomaterials in food and agriculture: an overview on their safety concerns and regulatory issues. *Crit Rev Food Sci Nutr*, **58**, 297-317.
- Jan H, Khan MA, Usman H, et al (2020). The *Aquilegia pubiflora* (Himalayan columbine) mediated synthesis of nanoceria for diverse biomedical applications. *RSC Advances*, **10**, 19219-231.
- Jan H, Shah M, Andleeb A, et al (2021). Plant-Based Synthesis of Zinc Oxide Nanoparticles (ZnO-NPs) Using Aqueous Leaf Extract of *Aquilegia pubiflora*: Their Antiproliferative Activity against HepG2 Cells Inducing Reactive Oxygen Species and Other In Vitro Properties. *Oxid Med Cell Longev*, **2021**, Article ID 4786227, **14**.
- Ji W, Zhu D, Chen Y, et al (2017). In-vitro cytotoxicity of biosynthesized zinc oxide nanoparticles towards cardiac cell lines of *Catla catla*. *Biomed Res*, **28**, 2262-6.
- Jiang J, Pi J, Cai J (2018). The advancing of zinc oxide nanoparticles for biomedical applications. *Bioinorganic Chem Appl*, **2018**, Article ID 1062562, 18 Pages.
- Kalim S, Nikalje APG (2017). A brief review on *Bauhinia variegata*: phytochemistry, antidiabetic and antioxidant potential. *Am J Pharm Tech Res*, **7**, 186-97.
- Kavitha MK, John H, Gopinath P, et al (2013). Synthesis of reduced graphene oxide-ZnO hybrid with enhanced optical limiting properties. *J Mater Chem C*, **23**, 3669-76.
- Khalil AT, Ayaz M, Ovais M, et al (2018). In vitro cholinesterase enzymes inhibitory potential and in silico molecular docking studies of biogenic metal oxides nanoparticles. *Inorg Nano-Met Chem*, **48**, 441-8.
- Khorsand Zak A, Majid WHA, Mahmoudian MR, et al (2013). Starch-stabilized synthesis of ZnO nanopowders at low temperature and optical properties study. *Adv Powder Technol*, **24**, 618-24.
- Kim KM, Kim TH, Kim HM, et al (2012). Colloidal behaviors of ZnO nanoparticles in various aqueous media. *J Toxicol Environ Health Sci*, **4**, 121-31.
- Konop M, Damps T, Misicka A, et al (2016). Certain aspects of silver and silver nanoparticles in wound care: a minireview. *J Nanomaterials*, **2016**, Article ID 7614753, 10 Pages.
- Koopman G, Reutelingsperger CP, Kuijten GA, et al (1994). Annexin V for flow cytometric detection of phosphatidylserine expression on B cells undergoing apoptosis. *Blood*, **84**, 1415-20.
- Lavanya R, Maheswari S, Harish G, et al (2010). Investigation of in-vitro anti-inflammatory, anti-platelet and anti-arthritis activities in the leaves of *Anisomeles malabarica* Linn. *Res J Pharm Biol Chem Sci*, **1**, 745-52.
- Mei L, Ping W, Wang ZY, et al (2012). GC-MS Analysis of Chemical Components in Seeds Oil from *Croton tiglium*. *J Chin Med Mater*, **35**, 1105.
- Modena MM, Rühle B, Burg TP, et al (2019). Nanoparticle characterization: what to measure?. *Adv Mater*, **31**, 1901556.
- Nagajyothi PC, Cha SJ, Yang IJ, et al (2015). Antioxidant and anti-inflammatory activities of zinc oxide nanoparticles synthesized using *Polygala tenuifolia* root extract. *J Photochem Photobiol B Biol*, **146**, 10-7.
- Nagajyothi PC, Sreekanth TVM, Tettey CO, et al (2014). Characterization, antibacterial, antioxidant, and cytotoxic activities of ZnO nanoparticles using *Coptidis Rhizoma*. *Bioorg Med Chem Lett*, **24**, 4298-4303.
- Nair SS, Kavrekar V, Mishra A (2013). In vitro studies on alpha amylase and alpha glucosidase inhibitory activities of selected plant extracts. *Eur J Exp Biol*, **3**, 128-32.
- Ojo M, Amoo A, Ayoade W, et al (2017). Physicochemical properties, fatty acid composition and antimicrobial potential of Turk's cap (*Croton penduliflorus*) seed oil. *Chem Sci Int J*, **20**, 1-7.
- Owade JO, Gachhiri CK, Abong GO (2019). Utilization of

- croton seed as a possible animal feed: a review. *Online J Anim Feed Res*, **9**, 178-86.
- Oyaizu M (1986). Studies on product of browning reaction prepared from glucose amine. *Jpn J Nutr*, **44**, 307-15.
- Oyedapo OO, Famurewa AJ (1995). Antiprotease and Membrane Stabilizing Activities of Extracts of Fagara Zanthoxyloides, Olax Subscorpioides and Tetrapleura Tetraptera. *Int J Pharmacogn*, **33**, 65-9.
- Ozkan E, Allan E, Parkin IP (2018). White-light-activated antibacterial surfaces generated by synergy between zinc oxide nanoparticles and crystal violet. *ACS Omega*, **3**, 3190-9.
- Paget GE, Barnes JM (1964). Toxicity tests. In: Laurance DR, Bacharach AL, editors. Evaluation of Drug Activities: Pharmacometrics, Vol 1. New York: Academic Press: pp 135-65.
- Parihar V, Raja M, Paulose R (2018). A brief review of structural, electrical and electrochemical properties of zinc oxide nanoparticles. *Rev Adv Mater Sci*, **53**, 119-30.
- Pfaffl MW (2001). A new mathematical model for relative quantification in real-time RT-PCR. *Nucleic Acids Res*, **29**, e45.
- Prieto P, Pineda M, Aguilar M (1999). Spectrophotometric quantitation of antioxidant capacity through the formation of a phosphomolybdenum complex: Specific application to the determination of vitamin E. *Anal Biochem*, **269**, 337-41.
- Rahman MM, Islam MB, Biswas M, et al (2015). In vitro antioxidant and free radical scavenging activity of different parts of Tabebuia pallida growing in Bangladesh. *BMC Res Notes*, **8**, 621-8.
- Rakmai J, Cheirsilp B, Mejuto JC, et al (2018). Antioxidant and antimicrobial properties of encapsulated guava leaf oil in hydroxypropyl-beta-cyclodextrin. *Ind Crop Prod*, **111**, 219-25.
- Sai Prassana CG, Karpaga S (2015). Comparative studies on the morphology of the stomach in the Insectivora. *Acta Theriol*, **12**, 223-44.
- Sanlioglu AD, Karacay B, Koksall IT, et al (2007). DcR2 (TRAIL-R4) siRNA and adenovirus delivery of TRAIL (Ad5hTRAIL) break down in vitro tumorigenic potential of prostate carcinoma cells. *Cancer Gene Ther*, **14**, 976-84.
- Selvarajan E, Mohanasrinivasan V (2013). Biosynthesis and characterization of ZnO nanoparticles using Lactobacillus plantarum VITES07. *Mater Lett*, **112**, 180-2.
- Senthilkumar N, Nandhakumar E, Priya PV, et al (2017). Synthesis of ZnO nanoparticles using leaf extract of Tectona grandis (L.) and their anti-bacterial, anti-arthritis, anti-oxidant and in vitro cytotoxicity activities. *N J Chem*, **41**, 10347-56.
- Shaban E, Salaheldin K, El sayed E, et al (2021). Evaluation of Acute Oral Toxicity of Zinc Oxide Nanoparticles in Rats. *Egypt J Chem*, **64**, 4591-4600.
- Singleton VL, Rossi JA (1965). Colorimetry of total phenolics with phosphomolybdic phosphotungstic acid reagents. *Am J Enol Vitic*, **16**, 144-58.
- Smima TP, Mathew J, Janardhanan KK, et al (2011). Antioxidant activity and toxicity profile of total triterpenes isolated from Ganoder malucidum (Fr.) P. Karst occurring in South India. *Environ Toxicol Pharm*, **32**, 438-46.
- Song Y, Yang J (2016). Preparation and in-vitro cytotoxicity of zinc oxide nanoparticles against osteoarthritic chondrocytes. *Tropical J Pharm Res*, **15**, 2321-7.
- Suganthi N, Sri Ramkumar V, Pugazhendhi A, et al (2018). Biogenic synthesis of gold nanoparticles from Terminalia arjuna bark extract: assessment of safety aspects and neuroprotective potential via antioxidant, anticholinesterase, and antiamyloidogenic effects. *Environ Sci Pollut Res Int*, **25**, 10418-33.
- Torres MCM, Assunção JC, Santiago GMP, et al (2008). Larvicidal and nematicidal activities of the leaf essential oil of Croton regelianus. *Chem Biodivers*, **5**, 2724-8.
- Vichai V, Kirtikara K (2006). Sulforhodamine B colorimetric assay for cytotoxicity screening. *Nat Protoc*, **1**, 1112-6.
- Vimala K, Sundarraj S, Paulpandi M, et al (2014). Green synthesized doxorubicin loaded zinc oxide nanoparticles regulates the Bax and Bcl-2 expression in breast and colon carcinoma. *Process Biochem*, **49**, 160-72.
- Wang J, Deng X, Zhang F, et al (2014). ZnO nanoparticle-induced oxidative stress triggers apoptosis by activating JNK signaling pathway in cultured primary astrocytes. *Nanoscale Res Lett*, **9**, 1-12.
- Wang Y, Pi C, Feng X, et al (2020). The influence of nanoparticle properties on oral bioavailability of drugs. *Int J Nanomedicine*, **15**, 6295-6310.
- Wickramaratne MN, Punchihewa J, Wickramaratne D (2016). In-vitro alpha amylase inhibitory activity of the leaf extracts of Adenanthera pavonina. *BMC Complement Altern Med*, **16**, 466.
- XiuLan W, MengYu G, Fang L, et al (2017). One-step green synthesis of bimetallic Fe/Ni nanoparticles by eucalyptus leaf extract: biomolecules identification, characterization and catalytic activity. *Chem Eng J*, **308**, 904-11.
- Yuvakkumar R, Suresh J, Nathanael AJ, et al (2014). Novel green synthetic strategy to prepare ZnO nanocrystals using rambutan (Nephelium lappaceum L.) peel extract and its antibacterial applications. *Mater Sci Eng C*, **41**, 17-27.
- Zia-Ul-Haq M, Shahid SA, Ahmad S, et al (2012). Antioxidant potential of various parts of Ferula assafoetida L. *J Med Plants Res*, **6**, 3254-8.



This work is licensed under a Creative Commons Attribution-Non Commercial 4.0 International License.